Computer Assisted Mechanics and Engineering Sciences, 9: 519–541, 2002.

Sensitivity analysis and material identification for activated smooth muscle[1]

Eduard Rohan and Robert Cimrman
University of West Bohemia, Faculty of Applied Sciences, Department of Mechanics
306 14 Plzeň, Czech Republic

(Received Februay 9, 2001)

The paper deals with the problem of material identification for smooth muscle tissue in activated, or passive states. In [17] a composite type mathematical model has been proposed describing the complexity of the tissue reduced to the networks of muscle and collagen fibres. The computational model is based on the total Lagrangian formulation with incompressibility of the bulk material. The problem of inflating vessels is considered in order to allow simulation of real experimental conditions and, thus, to determine constitutive parameters of muscle in active state. These parameters are identified also from hysteresis, or relaxation curves. The direct differentiation, or the adjoint systems techniques are applied to the sensitivity analysis. Results of numerical tests are given.

1. Introduction

Mathematical modelling of soft tissues belongs to the most complicated areas of the contemporary computational mechanics. There are several aspects that make the problem difficult. One of the main obstacles is the complex microstructure of soft tissues comprising entangled networks of fibrous components embedded in an amorphous phase, that can be characterized as a fluid with a very high viscosity. Usually, the tissue is subjected to large deformation so that, due to fibre reorientation and various interactions performing between the micro-components, the macroscopic properties of the tissue may change completely. In the case of muscle tissues the phenomenon of contraction and of the tonus generated dominates and brings another problem, as its properties strongly depend on the level of activation.

For developing macromodels of soft tissues an approach, which is based to a certain extent on the phenomenological theory of mixtures, is being used frequently, cf. [11, 17, 21, 22]. These models are defined in terms of constants, or parameters, which must be identified using experimental results obtained for a *macroscopic* specimen of the tissue. We note that related problems were studied in [14] for the Fung's uniaxial viscoelasticity model and by Humprey in [8] for a bi-axial test. Nowadays it is possible to get some experimental data describing behaviour of single micro-components (e.g. cells). However, such data can hardly be used to "calibrate" a macromodel, which does not reflect precisely how the micro-components are assembled in the structure.

This paper presents an approach to the material identification, which is based on optimization methods. We are concerned with the model of smooth muscle introduced in [17, 18], which treats the tissue in terms of the three constituents: the matrix, the passive fibres and the active fibres. In Sections 2–4 the constitutive laws for all of them are introduced. The problem of material identification is established in Section 6; the sensitivity analysis based alternatively on the direct differentiation, or the adjoint system methods is described in Section 7. In Section 5 mathematical modelling of inflated vessels is discussed. We formulate the problem for a deformable vessel interacting with

[1]This is an extended version of the article presented at the 8th International Conference on Numerical Methods in Continuum Mechanics, Liptovský Ján, Low Tatras, Slovakia, September 19–24, 2000.

an incompressible fluid. A quasi-static case is considered, when the inertia forces are neglected. The inflation problem is proposed to simulate experiments in conditions that are very close to physiological ones. Due to simplicity of the mathematical formulation it can be used for the identification. In Section 8 numerical examples including standard hysteresis and relaxation tests, as well as the inflation test are introduced for two cases: the identification of passive properties and identification of active properties.

2. Composite model

We shall consider the material composed of three basic components: the *active fibres* representing bundles of smooth muscle cells, the *passive fibres* representing collagen and elastin fibres and the *matrix* which corresponds to the amorphous extracellular substance. These components are supposed to occupy an infinitesimal volume according to the volume fractions denoted by ϕ^{a}, ϕ^f and ϕ^m respectively, so that

$$\phi^m + \phi^f + \phi^{\mathrm{a}} = 1\,. \tag{1}$$

In contrast to the theory of mixtures, both the fibrous phases are coupled kinematically with the matrix and, thus, cannot move separately. It is generally accepted that most of soft tissues, including smooth muscles, are incompressible. For treating the genuine incompressibility we use a mixed formulation in which the primary variables are displacements $\underline{u} = (u_1\,, u_2\,, u_3)$ and the pressure p. In the sequel we use the standard notation: $J = \det(F_{ij})$ is the Jacobian of the deformation gradient F and $C_{ij} = F_{ki}F_{kj}$ is the right Cauchy–Green deformation tensor.

In this paper we assume that the matrix, substituting the extracellular substance, is elastic. This simplification can be justified in the case of elastic arteries, that contain a large amount of elastin in the form of complex networks. On the other hand we shall consider only small contribution of the matrix to the mechanical behaviour of the tissue. A more sophisticated model (visco-elastic) is left for another opportunity.

In order to describe behaviour of the matrix we employ the neo-Hookean hyperelastic material, cf. [4], which is a special case of the Mooney–Rivlin model; the strain energy defined as $W^m = \frac{1}{2}\mu(J^{-2/3}C_{kk} - 3)$ is differentiated w.r.t. Green–Lagrange strain E_{ij} to get

$$S^m_{ij} = \frac{\partial W^m}{\partial E_{ij}} = \mu J^{-2/3}\left(\delta_{ij} - \frac{1}{3}C_{kk}C^{-1}_{ij}\right), \tag{2}$$

where μ is the shear modulus.

Including the effect of fibrous components, for the total second Piola–Kirchhoff stress in the composite we have

$$S_{ij} = -JC^{-1}_{ij}p + S^m_{ij} + \phi^f\tau^f_{ij} + \phi^{\mathrm{a}}\tau^{\mathrm{a}}_{ij}\,, \tag{3}$$

where τ^f_{ij} comprises tension in the passive fibres and τ^{a}_{ij} represents a tension produced by activated smooth muscle cells. Before we focus on describing behaviour of both the passive fibres and the active fibres we need to explain how these fibrous phases are incorporated in the model.

At any point of the material the fibres, both active and passive, are distributed in several *preferential directions*; the k-th one is defined by unit vector $\underline{\nu}^k = (\nu^k_1\,, \nu^k_2\,, \nu^k_3)$ related to the undeformed configuration. As the preferential directions of the active and passive fibres are independent in general, we consider index sets I^{a} and I^f, so that $k \in I^{\mathrm{a}} \cup I^f$. A quantity of fibres aligned with $\underline{\nu}^k$ is proportional to the volume fraction ϕ^k_{n}, where obviously $\sum_{k\in I^{\mathrm{n}}}\phi^k_{\mathrm{n}} = 1$ for $\mathrm{n} = \mathrm{a}, f$. Using the tensor

$$\omega^k_{ij} = \nu^k_i\nu^k_j \tag{4}$$

we can now express the tension stresses τ^{a}_{ij} and τ^{f}_{ij} through

$$\tau^{\mathrm{a}}_{ij} = \sum_{k\in I^{\mathrm{a}}} \phi^k_{\mathrm{a}} \tau^k_{\mathrm{a}} \omega^k_{ij}\,, \qquad \tau^{f}_{ij} = \sum_{k\in I^{f}} \phi^k_{f} \tau^k_{f} \omega^k_{ij}\,. \tag{5}$$

Above τ^k_{a} and τ^k_f are tensions which will be defined in the following text.

3. Passive fibres

The passive connective tissue comprises elastin and collagen fibres which both exhibit the quasi-elastic, or viscoelastic behaviour. In our model we approximate them using the uniaxial Kelvin (3-parametric) model of viscoelasticity with the discrete relaxation spectrum (i.e. structural damping sensitive to frequency of loading), see e.g. Section 7.6 of [5]. The *viscoelastic stress* τ^k (associated with the k-th preferential direction) is a function of the (nonlinear) *elastic response* σ^k and the internal stress-like variable q^k, such that

$$\tau^k = \sigma^k - q^k\,,$$
$$\dot{q}^k + \frac{1}{T_\epsilon} q^k = \frac{\gamma}{T_\epsilon}\sigma^k\,,$$

where T_ϵ is the relaxation time, γ is the relaxation parameter and $\dot{(\,)}$ denotes the time derivative. In [20], Chap. 10, the above model is called the *generalized relaxation model.* In the thermodynamic equilibrium $\dot{q}^k = 0$, see e.g. [3] for topics of the dissipation. Eliminating q^k we arrive at the following differential equation

$$\tau^k + T_\epsilon \frac{\mathrm{d}\tau^k}{\mathrm{d}t} = (1-\gamma)\left[\sigma^k + T_\sigma \frac{\mathrm{d}\sigma^k}{\mathrm{d}t}\right], \tag{6}$$

where T_σ is the creep time, $T_\sigma = T_\epsilon/(1-\gamma)$. From (6) one can obtain explicit (inverse) formula for $\sigma^k(t)$,

$$\sigma^k(t) = \frac{1}{1-\gamma}\left(\tau^k(t) - \gamma\int_{t_0}^{t} \exp\{-\beta(t-s)\}\,\frac{\mathrm{d}}{\mathrm{d}s}\tau^k(s)\,\mathrm{d}s\right), \tag{7}$$

where $\beta = (1-\gamma)/T_\epsilon \equiv (T_\sigma)^{-1}$.

We shall now introduce the *projection* of the Green–Lagrange strain, $E_{ij} = E_{ij}(\underline{u})$,

$$\epsilon^k(t) \equiv E_{ij}(\underline{u}(t))\,\omega^k_{ij}\,, \tag{8}$$

which expresses deformation of fibres aligned with the direction $\underline{\nu}^k$. The elastic response is given always by *instantaneous* strain $\epsilon^k(t)$. To capture the typical progressive stiffening of connective fibres, it is natural to use an exponential law for the definition of the elastic response, see [5],

$$\sigma^k(t) = D\exp\left\{\kappa(\epsilon^k(t) - \bar{\epsilon}^k_0)\right\} - \sigma_0\,. \tag{9}$$

In Eq. (9) D, κ and σ_0 are positive constants and $\bar{\epsilon}^k_0$ is the so called *relative slack length* of the k-th fibre.

In the literature the collagen fibres are reported to be tangled in helical bundles when the tissue is undeformed. As a consequence these fibres can transmit tension only after their straightening, while in compression they cannot transmit any load. This behaviour results in the fact that the bulk stiffness of the composite material increases as the stretch progresses. In [17] the following assumptions were considered:

1. compression of the composite material in the "direction" of the fibres does not affect the bulk behaviour; the same holds for a fibre which is unloaded;
2. in the context of the assumed *viscoelasticity* of the fibres, the deformation of a released (unloaded) fibre can develop independently of that of the bulk material (matrix).

These properties of the fibre-structure interaction can be described mathematically using complementarity relations

$$\begin{aligned} &\varepsilon_f^k(t) \geq \epsilon^k(t) - \bar{\epsilon}_0^k\,, \\ &\tau^k(t) \geq 0\,, \\ &\tau^k(t) \cdot (\varepsilon_f^k(t) - \epsilon^k(t) + \bar{\epsilon}_0^k) = 0\,, \end{aligned} \tag{10}$$

where τ_f^k and ε_f^k denote the tension and the strain of the k-th fibre, respectively.

To summarize, we note, that Eqs. (6), (9) and (10) constitute an implicit relation between ϵ^k and τ^k which is imposed at any time t. As a further step we consider a time discretization employed throughout the next paper. Let $[t_0, T] = \cup_{n=0}^{n_T}[t_n, t_{n+1}]$ where $t_{n+1} = t_n + \Delta t$. A quantity $y(t)$ is approximated at t_n by $y^{(n)}$. In the rest of this Section for brevity we drop the superscript k associated with the preferential directions. Using the trapezoidal rule to discretize in time the convolution of Eq. (7) and recalling Eqs. (8) and (9), we obtain a general recursive formula for τ: Given the *history* parameter $h^{(n)}$, see Eq. (13), we first compute the *trial tension* $\tilde{\tau}^{(n+1)}$,

$$\tilde{\tau}^{(n+1)} = \frac{1}{c}\left[(1-\gamma)\,\sigma(\underline{u}^{(n+1)}) + \gamma\left(\exp\{-\beta\Delta t\}\,h^{(n)} - \exp\left\{-\frac{\beta}{2}\Delta t\right\}\tau^{(n)}\right)\right], \tag{11}$$

where $c = 1 - \gamma\exp\{-\frac{\beta}{2}\Delta t\}$. The complementarity relations (10) now yield the *projection step*

$$\tau^{(n+1)} = \max\{0,\ \tilde{\tau}^{(n+1)}\}. \tag{12}$$

With $\tau^{(n+1)}$ we can update the history parameter,

$$h^{(n+1)} = \exp\{-\beta\Delta t\}h^{(n)} + \exp\left\{-\frac{\beta}{2}\Delta t\right\}(\tau^{(n+1)} - \tau^{(n)})\,. \tag{13}$$

For initialization of (11) and (13) we put

$$\begin{aligned} &\tilde{\tau}^{(0)} = (1-\gamma)\,\sigma(\underline{u}^{(0)})\,, \\ &h^{(0)} = 0\,. \end{aligned}$$

The above computation can be applied to any elastic response function σ. In the case of exponential law (9) we have

$$\sigma^{(n+1)} = D\exp\left\{\kappa\left(E_{ij}(\underline{u}^{(n+1)})\omega_{ij} - \bar{\epsilon}_0\right)\right\} - \sigma_0\,. \tag{14}$$

We note that the fibre strain, ε_f, is the internal variable. If $\tau^{(n+1)} = \tilde{\tau}^{(n+1)}$, then $\varepsilon_f^{(n+1)}$ can be computed as $E_{ij}(\underline{u}^{(n+1)})\omega_{ij} - \bar{\epsilon}_0$.

4. Simplified model of active fibres

In smooth muscle the process of activation and muscle contraction differs from that known for striated muscle. On the other hand for both the types of muscle tissue the essential features are common: the force is generated by actin-myosin cross-bridges activated by calcium ions; the force of contraction is disproportional to the velocity of contraction (during fibre shortening).

In this paper we consider a simplified model of active fibres which was presented in [17]. In a context of this model the active fibre is taken as a generator of tension τ_a. We assume that τ_a depends on

1. *activation* factor A_{Ca}, which is related to intracellular calcium ions concentration,
2. local *strain* ϵ (in a particular direction of the fibre),
3. local *strain rate* $\dot{\epsilon}$ (in a particular direction of the fibre).

As we are interested in quasi-static behaviour of the tissue, we can neglect transient effects associated with development of the muscle activity, which may be important for studying short period events, cf. [15]. It should be remarked, that for a correct description of the transient phenomena the sliding cross-bridge models should be used, see [1, 9, 23] and the references cited therein. A more sophisticated model of activation specific to the smooth muscle was presented by the authors in [3].

The definition of τ_{a}^k associated with the k-th preferential direction has the following form,

$$\tau_{\mathrm{a}}^k(\epsilon^k, \dot{\epsilon}^k, \alpha) = \eta\dot{\epsilon}^k + A_{\mathrm{Ca}}^k \bar{f}_{\max} \exp\left\{-\left(\frac{\epsilon^k - \varepsilon_{\mathrm{opt}}}{s}\right)^2\right\} \exp\left\{\vartheta \min\{0; \dot{\epsilon}^k\}\right\}. \tag{15}$$

The first term in the right hand side of Eq. (15) is the passive viscosity resistance, whereas the second term corresponds to the activated tension. The parameter $\varepsilon_{\mathrm{opt}}$ is the optimal relative strain for which a maximum generated force can be achieved. All parameters involved in Eq. (15) are summarized in Table 1. In Fig. 1 we illustrate how the activated tension depends on strain rate. We remark that for a correct description of the so called *"Latch mechanism"*, see e.g. [6], a more sophisticated model of activation should be considered, as mentioned above.

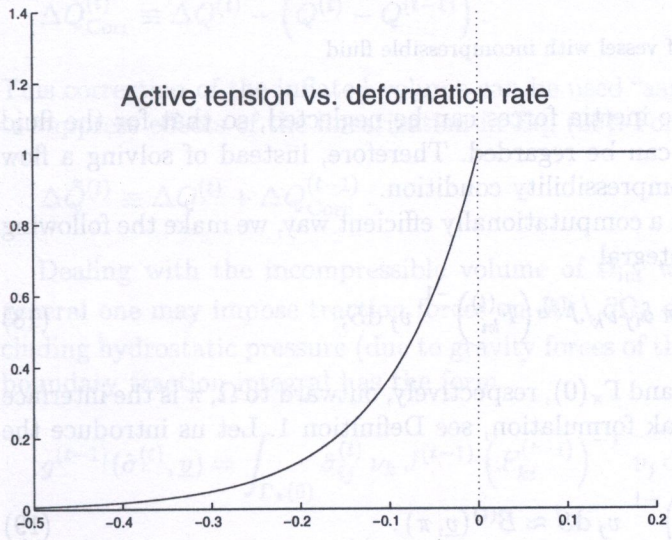

Table 1

$\bar{f}_{\max}$	maximum tension generated
$\varepsilon_{\mathrm{opt}}$	optimal strain
s	sensitivity to actual strain
ϑ	sensitivity to actual strain rate
η	viscosity (passive)

Fig. 1. Dependence of strain rate on active tension

For numerical simulation we shall employ the discretized form of Eq. (15). Using the backward finite differences we obtain

$$\tau_{\mathrm{a}}^{k,(n+1)} = \frac{\eta}{\Delta t}\left(\epsilon^{k,(n+1)} - \epsilon^{k,(n)}\right) + A_{\mathrm{Ca}}\, \bar{f}_{\varepsilon}^{k,(n+1)} \exp\left\{\frac{\vartheta}{\Delta t} \min\left\{0; \epsilon^{k,(n+1)} - \epsilon^{k,(n)}\right\}\right\} \tag{16}$$

for all preferential directions $k \in I^{\mathrm{a}}$ where

$$\bar{f}_{\varepsilon}^{k,(n+1)} = \bar{f}_{\max} \exp\left\{-\left(\frac{\epsilon^{k,(n+1)} - \varepsilon_{\mathrm{opt}}}{s}\right)^2\right\}. \tag{17}$$

We remark that $\tau_{\mathrm{a}}^{k,(n+1)}$ is a nonsmooth function of $\epsilon^{k,(n+1)}$ due to the dependence of the contractive tension on the shortening rate.

5. Model of inflated vessel – weak formulation

In preceding sections we introduced the constitutive relations describing behaviour of both active and passive fibres. These constitutive relations has already been discretized in time and, to express S_{ij} defined in Eq. (3), the passive and the active tensions in Eq. (5) can be defined using Eqs. (12) and (16), respectively. As the result, the state of the deformed configuration at an instant t_{n+1} is determined explicitly in terms of displacements $\underline{u}^{(n+1)}$ and of the pressure $p^{(n+1)}$. Throughout the following paper we use the notation $^{(t)}$ instead of $^{(n)}$.

We shall now focus on defining a quasi-static *interaction problem* which will be used for modelling hollow organs. We consider an open bounded domain $\mathcal{O}^{(t)} \subset \mathbb{R}^3$ and its decomposition $\mathcal{O}^{(t)} = \Omega^{(t)} \cup \Omega_{\rm int}^{(t)} \cup \Gamma_\pi^{(t)}$. The domain $\Omega^{(t)}$ is occupied by the deformed tissue at time t and $\Omega_{\rm int}^{(t)}$ is a bounded cavity filled with an incompressible (inviscid) fluid, see Fig. 2. $\Gamma_\pi^{(t)}$ is the interface where the vessel $\Omega^{(t)}$ is loaded by the pressure π. For treating "(plane) symmetric" problems we also introduce the boundary Γ_s. On the "exterior" surface $\partial\Omega \setminus (\overline{\Gamma_s \cup \Gamma_\pi}) = \overline{\partial\Omega_u \cup \partial\Omega_\sigma}$ usual Dirichlet, or Neumann type boundary conditions are imposed.

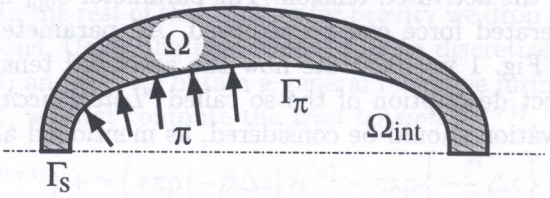

Fig. 2. Interaction of vessel with incompressible fluid

In the case of quasi-static deformation the inertia forces can be neglected, so that for the fluid in the cavity $\Omega_{\rm int}$ only its incompressibility can be regarded. Therefore, instead of solving a flow problem in $\Omega_{\rm int}$, we merely consider the incompressibility condition.

In order to treat the interaction problem in a computationally efficient way, we make the following simplification. We define interface traction integral

$$\mathcal{B}^{(t)}(\underline{v},\pi) \equiv \int_{\Gamma_\pi(t)} \pi\, \delta_{ij}\, n_i^{(t)} v_j \,\mathrm{d}S = \int_{\Gamma_\pi(0)} \pi\, \delta_{ij}\, \nu_k\, J^{(t)} \left(F_{ki}^{(t)}\right)^{-1} v_j \,\mathrm{d}S, \tag{18}$$

where $n_i^{(t)}$, ν_i are unit normal vectors of $\Gamma_\pi(t)$ and $\Gamma_\pi(0)$, respectively, outward to Ω, π is the interface pressure and $\underline{v}$ is the test function of the weak formulation, see Definition 1. Let us introduce the approximation

$$b^{(t-1)}(\underline{v},\pi) \equiv \int_{\Gamma_\pi(0)} \pi\, \delta_{ij}\, \nu_k\, J^{(t-1)} \left(F_{ki}^{(t-1)}\right)^{-1} v_j \,\mathrm{d}S \approx \mathcal{B}^{(t)}(\underline{v},\pi)\,. \tag{19}$$

As a further step we define the linearized incompressibility condition. Let the deformation of the whole structure $\mathcal{O}$ be described by a continuous displacement field $\underline{u}$. For the increment $\Delta\underline{u} = \underline{u}^{(t)} - \underline{u}^{(t-1)}$ let

$$\mathrm{div}\Delta\underline{u} = 0 \qquad \text{in} \quad \Omega_{\rm int}^{(t-1)}, \tag{20}$$

hold weakly in $L_2(\Omega_{\rm int}^{(t-1)})$ i.e.

$$\int_{\Omega_{\rm int}^{(t-1)}} \mathrm{div}\Delta\underline{u}\, q \,\mathrm{d}x = 0 \qquad \forall q \in L_2\left(\Omega_{\rm int}^{(t-1)}\right). \tag{21}$$

In fact we only need to have Eq. (21) satisfied for any $\bar{q} = \textit{constant}$ in $\Omega_{\rm int}^{(t-1)}$. Then, using the Gauss–Ostrogradski theorem one obtains the approximate incompressibility condition, see Eq. (19),

$$0 = \bar{q} \int_{\Gamma_\pi(0)} \delta_{ij}\, \nu_k\, J^{(t-1)} \left(F_{ki}^{(t-1)}\right)^{-1} \Delta u_j \,\mathrm{d}S = b^{(t-1)}(\Delta\underline{u},\bar{q})\,. \tag{22}$$

Remark 1. It is worth noting that the boundary traction integral (19) and the linearized incompressibility condition (22) are defined in terms of the same "bilinear" form $b^{(t-1)}(\underline{w}, \theta)$, where $\underline{w}$ is a displacement variable and θ is a constant. This is important for symmetry of an "extended stiffness matrix" introduced in Eq. (38).

If the internal bulk volume is supplied with the volume rate $\dot{Q}(t)$, instead of Eq. (22) we consider inflation of the vessel as follows. The fluid supplied in time interval $(t - \Delta t, t)$ is denoted by $\Delta Q^{(t)}$. Now the linearized conservation of volume can be expressed as

$$b^{(t-1)}(\underline{u}^{(t)}, 1) = b^{(t-1)}(\underline{u}^{(t-1)}, 1) - \underbrace{\Delta Q^{(t)}}_{\text{Source}} . \tag{23}$$

(Note that the minus above results from ν_k being the outward normal of Ω.)

Remark 2. The volume of $\Omega_{\text{int}}^{(t)}$ can easily be determined using boundary integral

$$Q^{(t)} = \int_{\Omega_{\text{int}}(t)} \mathrm{d}x = \frac{1}{3} \int_{\partial\Omega_{\text{int}}(t)} \underline{x}^{(t)} \cdot (-\underline{n}^{(t)}) \, \mathrm{d}S, \tag{24}$$

which is used to compute the correction source volume

$$\Delta Q_{\text{Corr}}^{(t)} \equiv \Delta Q^{(t)} - \left(Q^{(t)} - Q^{(t-1)} \right). \tag{25}$$

This correction of the inflated volume can be used "asynchronously" in subsequent time increments to suppress effects of the linearization in Eq. (20). For this we define

$$\Delta \tilde{Q}^{(t)} \equiv \Delta Q^{(t)} + \Delta Q_{\text{Corr}}^{(t-1)} . \tag{26}$$

Dealing with the incompressible volume of Ω_{int} we introduced boundary tractions on Γ_π. In general one may impose traction forces on $\partial\Omega \setminus \partial\Omega_u$ defined in terms of the Cauchy stress $\hat{\sigma}_{ij}^{(t)}$, including hydrostatic pressure (due to gravity forces of the fluid in Ω_{int}) acting on Γ_π. The "linearized" boundary traction integral has the form

$$g^{(t-1)}(\hat{\sigma}^{(t)}, \underline{v}) = \int_{\Gamma_\pi(0)} \hat{\sigma}_{ij}^{(t)} \nu_k J^{(t-1)} \left(F_{ki}^{(t-1)} \right)^{-1} v_j \, \mathrm{d}S , \tag{27}$$

where in this paper we consider

$$\hat{\sigma}_{ij}^{(t)} \equiv -p_g^{(t)} \delta_{ij} . \tag{28}$$

We shall now focus on defining the weak form of the *interaction subproblem*. The following admissibility sets are considered: $V_0 \equiv \left\{ \underline{v} \in [H(\Omega^{(0)})]^3 \mid \underline{v} = \underline{0} \text{ on } \partial\Omega_u^{(0)} \right\}$ and $V^{(t)} \equiv \left\{ \underline{v} \in [H(\Omega^{(0)})]^3 \mid \underline{v} = \underline{d}^{(t)} \text{ on } \partial\Omega_u^{(0)} \right\}$, where $\underline{d}^{(t)}$ are displacements prescribed on the boundary and H is the "abstract" functional space, see Remark 3.

Remark 3. In this paper we do not discuss any aspect of existence and uniqueness of solutions to the problem defined in Definition 1. In literature, see e.g. [2, 13], a simpler case of hyperelastic materials has been analyzed using the theory of locally monotone operators and poly-convex functions. The space H introduced above belongs to the class of Sobolev spaces $W^{1,p}$ with the exponent $p > 2$.

Definition 1. (Inflation subproblem) Given $h^{k,(t-1)}$, $\tau_f^{k,(t-1)} \in L_2(\Omega_0)$, $k \in I^f$ (see (11), (13)), the boundary tractions $\hat{\sigma}_{ij}^{(t)} \in L_2(\partial\Omega^{(t-1)} \setminus \partial\Omega_u^{(t-1)})$ and the (corrected) volume influx $\Delta\tilde{Q}^{(t)}$, see Eq. (26), find $\underline{u}^{(t)} \in V^{(t)}$, $p^{(t)} \in L_2(\Omega^{(0)})$, and the interface pressure $\pi^{(t)} \in \mathbb{R}$, so that

$$\mathcal{F}(\underline{u}^{(t)}, p^{(t)}, \underline{v}) + b^{(t-1)}(\underline{v}, \pi^{(t)}) = g^{(t-1)}(\hat{\sigma}^{(t)}, \underline{v}) \qquad \forall\, \underline{v} \in V_0\,, \tag{29}$$

$$\mathcal{G}(\underline{u}^{(t)}, q) = 0 \qquad \forall\, q \in L_p(\Omega^{(0)})\,, \tag{30}$$

$$b^{(t-1)}(\underline{u}^{(t)}, 1) = b^{(t-1)}(\underline{u}^{(t-1)}, 1) - \Delta\tilde{Q}^{(t)}\,, \tag{31}$$

where

$$\mathcal{F}(\underline{u}, p, \underline{v}) \equiv \int_{\Omega_0} S_{ij}\left(\underline{u}, p, \tau_f^{k,(t-1)}, h^{k,(t-1)}\right) \delta_u E_{ij}(\underline{u}; \underline{v})\, \mathrm{d}\Omega\,,$$

$$\mathcal{G}(\underline{u}, q) \equiv \int_{\Omega_0} (1 - J(\underline{u}))\, q\, \mathrm{d}\Omega\,,$$

and $\delta_u E_{ij}(\underline{u}; \underline{v})$ is the differential of the Green strain $E_{ij}(\underline{u})$.

Thus, the subproblem of Definition 1 comprises the *balance of forces* equation (29) involving the interface integral, the *incompressibility condition* (30) imposed on the *bulk composite material*, and the *approximate conservation of volume equation* (31) related to the volume of the cavity.

In Section 6 the identification problem will be introduced with the *state problem* defined in terms of subproblems of Definition 1 discretized in space using mixed finite elements. From now on, let us denote by u the displacement vector, by p the vector of hydrostatic pressures in the composite (at the pressure nodes). Further let τ be the vector of tensions in the passive fibres and h be the vector of the history variables, both defined at the quadrature points. Still by π we denote the value of the pressure in the internal volume.

The set $\{y^{(t)}\}_{t=1}^n$, where $y^{(t)} = (u, p, \pi, \tau, h)^{(t)} \in \mathbb{R}^M$ is called the *extended solution of the discretized state problem* if it satisfies the set of nonlinear equations (here presented in an abstract form)

$$\Phi^{(t)}(y^{(t-1)}, y^{(t)}) = 0\,, \qquad t = 1, \ldots, n\,, \tag{32}$$

for a given initial condition $y^{(0)}$. The block structure of the *state function* $\Phi^{(t)} \in \mathbb{R}^M$ corresponds to its restriction to a single finite element e,

$$\Phi_e^{(t)} \equiv \begin{bmatrix} \mathcal{U}_e & \text{(equilibrium)} \\ \mathcal{P}_e & \text{(incompressibility)} \\ \mathcal{V}_e & \text{(interaction)} \\ \mathcal{T}_e & \text{(fibre tension)} \\ \mathcal{H}_e & \text{(history)} \end{bmatrix} = (\text{restriction}_e)\, \Phi^{(t)} \equiv \begin{bmatrix} \mathcal{U} \\ \mathcal{P} \\ \mathcal{V} \\ \mathcal{T} \\ \mathcal{H} \end{bmatrix}, \tag{33}$$

where the length of the (column) vectors $\mathcal{U}_e$ and $\mathcal{P}_e$ is the number of d.o.f. per element and the number of the pressure nodes per element, respectively. In Eq. (33) the "block" $\mathcal{V}$ is the discretized form of the (single) volume conservation equation (31). The lengths of both $\mathcal{T}_e$ and $\mathcal{H}_e$ are the number of preferential directions $\times$ number of quadrature points per element.

In order to give a more detailed information about the structure of $\Phi_e^{(t)}$ in Eq. (33), we need the following notation. By $\underline{\xi}^q$ we denote the quadrature point of a reference element T_R^e, W_q is the weight. There are n_Q quadrature points per each element. By $\underline{\zeta}^q$ we denote the quadrature points on faces ∂T_R^e. In analogy, W_q^S is the quadrature weight on ∂T_R^e. Let I_{QS}^e and $I_{QS\pi}^e$ be the set of all such quadrature points which are associated with boundaries $\partial\Omega \setminus \partial\Omega_u$ and Γ_π, respectively. Notation $(\cdot)|_q$ indicates evaluation of the $(\cdot)$ at $\underline{\xi}^q$. Further J_0 is the Jacobian of the mapping between the

(unit) reference and the spatial element, J_{S0} has analogical meaning, but is associated with the faces. The blocks in Eq. (33) have the following structure,

$$\begin{aligned}
\mathcal{U}_e \equiv & \sum_{q=1}^{n_Q} \mathbf{B}(\underline{\xi}^q, u)^T \cdot \mathbf{s}(\underline{\xi}^q, \mu, u, p, \tau)\, J_0(\underline{\xi}^q)\, W^q \\
& + \pi \sum_{q \in I^e_{QS\pi}} \boldsymbol{\chi}^T(\underline{\zeta}^q) \cdot \left[\mathbf{F}^{-T}(\underline{\zeta}^q) \cdot \boldsymbol{\nu}(\underline{\zeta}^q)\right]^{(t-1)} J_{S0}(\underline{\zeta}^q)\, W^q_S \\
& - \sum_{q \in I^e_{QS}} \boldsymbol{\chi}^T(\underline{\zeta}^q) \cdot \hat{\boldsymbol{\sigma}}(\underline{\zeta}^q) \cdot \left[\mathbf{F}^{-T}(\underline{\zeta}^q) \cdot \boldsymbol{\nu}(\underline{\zeta}^q)\right]^{(t-1)} J_{S0}(\underline{\zeta}^q)\, W^q_S , \\
\mathcal{P}_e \equiv & \sum_{q=1}^{n_Q} \left(1 - J(\underline{\xi}^q, u)\right) \boldsymbol{\psi}(\underline{\xi}^q)\, J_0(\underline{\xi}^q)\, W^q , \\
\mathcal{V}_e \equiv & \sum_{q \in I^e_{QS\pi}} \left[\boldsymbol{\nu}^T(\underline{\zeta}^q) \cdot \mathbf{F}^{-1}(\underline{\zeta}^q)\right]^{(t-1)} \cdot \boldsymbol{\chi}(\underline{\zeta}^q) \cdot \left(\mathbf{u}^{(t)} - \mathbf{u}^{(t-1)}\right) J_{S0}(\underline{\zeta}^q)\, W^q_S , \\
\mathcal{T}_e \equiv & \tau_k|_q - \frac{1}{c} \max\left\{0 \mid \gamma_\infty \left(\exp\left\{\kappa(\epsilon^k - \bar{\epsilon}^k_0)\right\} - 1\right) + \gamma\left(h_k^{(t-1)} - b\tau_k^{(t-1)}\right)\right\}\Big|_q , \\
\mathcal{H}_e \equiv & h_k|_q - a h_k^{(t-1)}\Big|_q - b\left(\tau_k - \tau_k^{(t-1)}\right)\Big|_q , \quad \forall\, q = 1, \ldots, n_Q , \quad \forall\, k \in I^f ,
\end{aligned} \tag{34}$$

where $\mathbf{B}$ is the matrix connecting the virtual change in strain to virtual displacements, $\mathbf{s}$ is the stress vector; J is determinant of the deformation gradient $\mathbf{F}$, $\boldsymbol{\nu}$ is the outward normal to the face, $\boldsymbol{\chi}$ and $\boldsymbol{\psi}$ comprise the basis functions for the displacement and the pressure approximation, respectively; $\hat{\boldsymbol{\sigma}}$ is the traction defined in Eq. (28). We use abbreviations $a = \exp\{-\beta\Delta t\}$, $b = \exp\{-\beta\Delta t/2\}$, $c = 1 - \gamma b$. In the definition of $\mathcal{T}_e$ by ϵ^k we denote the projected strain corresponding to $\underline{u}$, see Eq. (8).

It is worth noting that values of the element restriction of the interaction term of $\mathcal{U}_e$ are non-zero only if a face of the particular element lies on the interface Γ_π. An analogous statement holds for $\mathcal{V}_e$.

Remark 4. The system (32) can be solved by the Newton–Raphson iterations. It is obvious, that Eq. (32) can be reduced on substituting $\tau_k|_q$ and $h_k|_q$ from Eq. (34) into the stress $\mathbf{s}$ evaluated at the quadrature point $\underline{\xi}^q$, and then "cutting off" the last two blocks $\mathcal{T}$ and $\mathcal{H}$. However, in order to derive sensitivity formulae (the adjoint system method) for the identification problem, see Sections 6 and 7, the extended system must be considered, cf. [19]. Such treatment is needed because of the recurrent definition of the viscoelastic history parameter h, see Section 3.

The linear subproblems were derived in [17] for a standard case without treating inflation of the cavity. The tangent stiffness modulus, which is needed for assembling the stiffness matrix associated with FEM discretized form of Eq. (29), is given by (after the substitution noted in Remark 4)

$$\begin{aligned}
D_{ijkl} \equiv & a_1 C^{-1}_{ij} C^{-1}_{kl} + a_2 \left(\delta_{ij} C^{-1}_{kl} + C^{-1}_{ij} \delta_{kl}\right) + a_3 \left(C^{-1}_{ik} C^{-1}_{jl} + C^{-1}_{il} C^{-1}_{jk}\right) \\
& + \sum_{r \in I^a} b^r_a\, \omega^r_{ij}\, \omega^r_{kl} + \sum_{r \in I^f} b^r_f\, \omega^r_{ij}\, \omega^r_{kl} ,
\end{aligned} \tag{35}$$

where, cf. [4],

$$\begin{aligned}
a_1 &= \frac{2}{9}\mu\, C_{ii} \det(C)^{-1/3} - p \det(C)^{1/2} , \\
a_2 &= -\frac{2}{3}\mu \det(C)^{-1/3} , \\
a_3 &= \frac{1}{3}\mu\, C_{ii} \det(C)^{-1/3} + p \det(C)^{1/2} .
\end{aligned}$$

Differentiating the tension in the r-th passive fibre (see Section 3) one obtains

$$b_f^r \equiv \begin{cases} 0 & \text{if } \tau_f^r = 0\,, \\ \phi^f \phi_f^r(\gamma_\infty/c)\,\kappa\, \exp\left\{\kappa(\epsilon^{r,(t+1)} - \bar{\epsilon}_0^r)\right\} & \text{otherwise}\,, \end{cases} \tag{36}$$

and for the tension in the r-th active fibre (see Section 4)

$$b_{\mathrm{a}}^r \equiv \phi^{\mathrm{a}} \phi_{\mathrm{a}}^r \left[\frac{\eta}{\Delta t} + \alpha \exp\left\{ \frac{\vartheta}{\Delta t} \min\left\{0; \epsilon^{r,(t+1)} - \epsilon^{r,(t)}\right\}\right\} \right.$$
$$\left. \cdot \left(\frac{\mathrm{d}}{\mathrm{d}\epsilon} \bar{f}_\varepsilon^{r,(t+1)} + \bar{f}_\varepsilon^{r,(t+1)} \cdot \frac{\vartheta}{\Delta t} \max\left\{0; -\mathrm{sgn}(\epsilon^{r,(t+1)} - \epsilon^{r,(t)})\right\}\right)\right]. \tag{37}$$

In our case involving the inflation problem the linear subproblems associated with the Newton–Raphson iterations are extended by the approximate volume conservation equation (31). They have the following form:

$$\begin{bmatrix} K & P^T & \hbar \\ P & 0 & 0 \\ \hbar^T & 0 & 0 \end{bmatrix} \begin{pmatrix} \Delta u \\ \Delta p \\ \Delta \pi \end{pmatrix} = \begin{pmatrix} f \\ g \\ q \end{pmatrix}. \tag{38}$$

Above K is the stiffness matrix, P is called the pressure matrix and $\hbar$ is called the traction operator (vector). The right-hand side vector in Eq. (38) is called the *out-of-balance* vector, or the residual vector associated with blocks $\mathcal{U}, \mathcal{P}$ and $\mathcal{V}$ of Eq. (33). Due to the approximations employed in Eqs. (19) and (20), see Remark 1, the linear subproblems have a symmetric matrix, so that the Stokes problem solver, as discussed e.g. in [17], can be used to compute increments Δu, Δp, and $\Delta \pi$.

6. Identification of constitutive parameters

The model of smooth muscle presented in this paper is defined using many material parameters. Due to the large nonlinearity embedded in the model its response may change considerably, when changing values of some of these parameters. Therefore, a proper setting of the parameters is essential for applicability of the model when dealing with complex structural problems in biomechanics.

In this section we present an optimization-based approach to the material identification problem. A specimen of the smooth muscle undergoes an experiment, so that one obtains a time record of a measured quantity (e.g. loading force, or stretch, etc.) which can also be computed by numerical simulation. Then a criterion function is assigned to the time record. The criterion function is then minimized using methods of mathematical optimization to obtain some proper material parameters.

The *microstructure* of the particular specimen can be studied performing morphological, histochemical and stereological analysis. In the context of our smooth muscle model it means that the volume fractions of all components and also the preferential directions of fibres can be defined at several cross-sections of the specimen. The identification procedure then attempts to find constitutive parameters describing behaviour of the muscle in *resting state*, when muscle fibres are not activated, and in *activated* state (for a given level of activation). We consider the following identification parameters α associated with:

- **resting state** (muscle fibres not activated)

α_1	μ	shear modulus of matrix	
α_2	γ_∞	relaxation stiffness	$\gamma_\infty = (1-\gamma)D$
α_3	κ	exponential power of fib.	
α_4	β	inverse creep time	$\beta = (1-\gamma)/T_{\mathrm{relax}}$
α_5	γ	relaxation parameter	
α_{k+5}, $k = 1,2,3$	$\bar{\epsilon}_0^k$	slack length for passive fibres	

- **activated state**

α_1^*	$\bar{f}_{\max}$	maximal tension generated
α_2^*	ε_{opt}	optimal strain
α_3^*	s	sensitivity to actual strain
α_4^*	ϑ	sensitivity to actual strain rate

Let a sequence of measured quantities $\bar{\varphi}_i$ at time levels $t_i, i \in \mathcal{I} \subset \{1, \ldots, n\}$, $m = \text{card}(\mathcal{I})$ be given. For each $\bar{\varphi}_i$ its counterpart $\varphi_i(\alpha, y^{(i)})$ can be evaluated with $y^{(i)}$, the solution of the state problem (32). The objective function takes the general form

$$F(\alpha) \equiv \frac{1}{2} \sum_{i \in \mathcal{I}} \left(\varphi_i(\alpha, y^{(i)}) - \bar{\varphi}_i \right)^2 . \tag{39}$$

The identification problem is defined as follows: Find $\bar{\alpha} \in U_{ad} \subset \mathbb{R}^N$, so that

$$\bar{\alpha} = \arg\min_{\alpha} \left\{ F(\alpha, \mathbf{y}(\alpha)) \;\mid\; \alpha \in U_{ad} \subset \mathbb{R}^N, \quad \mathbf{y}(\alpha) \equiv \{y^{(i)}\}_{i=1}^n \text{ solves the state problem (32)} \right\}, \tag{40}$$

where U_{ad} is the admissibility set defined in terms of box constraints. As can be seen from Eq. (39), the problem in Eq. (40) belongs to a class of nonlinear least squares problems, with non-convex objective function (in α). Moreover, because of the projection involved in the constitutive relations (12) and (16), the objective function is also nonsmooth, in general.

In our numerical examples we consider the following identification problems.

1. **Isometric Relaxation / Hysteresis**. A specimen, fixed in the apparatus, undergoes uniaxial stretch, while the loading force $\bar{f}(t_i)$ is measured at m time levels. The diagram of stretch-program is illustrated in Fig. 3. For evaluation of the loading force numerically, we define a cross-sectional surface $\mathcal{S}_0$ in the reference configuration and the unit vector $\underline{\nu}$ normal to $\mathcal{S}_0$. In time

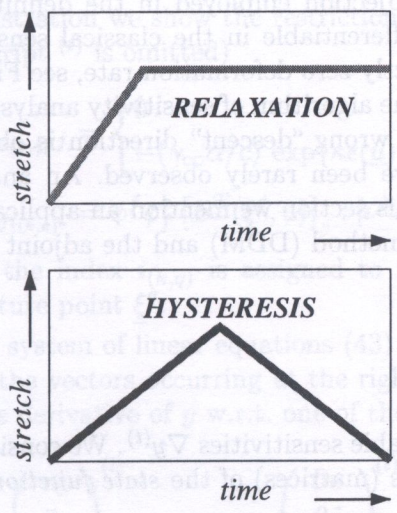

Fig. 3. Stretch program for relaxation and hysteresis tests

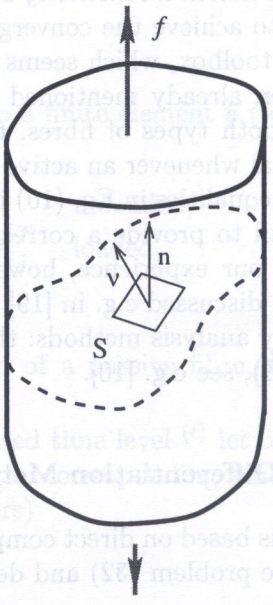

Fig. 4. Computation of loading force in stretched specimen

the surface $\mathcal{S}_0$ changes to $\mathcal{S}(t)$. Denoting by $\underline{n}$ the direction (fixed), in which the specimen is being loaded, see Fig. 4, the objective function of the type (39) takes the following form

$$F_1(\alpha) \equiv \frac{1}{2} \sum_{i \in \mathcal{I}} \left(\int_{\mathcal{S}_0} n_j \, F^{(i)}_{jk} \, S^{(i)}_{kl} \, \nu_l \, \mathrm{d}\mathcal{S} - \bar{f}(t_i) \right)^2 , \tag{41}$$

where the notation of Section 2 is employed. Obviously, in this test the interaction, as described in Section 5, is not considered, so that the state problem involves neither Eq. (31), nor the interface traction integral in Eq. (29).

2. **Inflation of vessel.** We have a vessel (tube, balloon) fitted into an appropriate apparatus, so that a bounded volume (the cavity) is formed. Then injecting subsequently amounts of fluid into the cavity, the pressure $\bar{\pi}(t)$ in the fluid is measured in time. The "inflation program" used can be analogous to the diagrams in Fig. 3, where the stretch is replaced by the inflated volume. The objective function is very simple in this case,

$$F_2(\alpha) \equiv \frac{1}{2} \sum_{i \in \mathcal{I}} \left(\pi^{(i)} - \bar{\pi}(t_i) \right)^2 , \tag{42}$$

as $\pi^{(i)} \approx \pi(t_i)$ is one of the state variables of the inflation problem.

The objective functions defined above can be minimized numerically using the Levenberg–Marquardt method with a step length reduction. The search direction $\Delta\alpha$ (column vector) is determined from the "optimality" condition $\nabla_{\Delta\alpha} \tilde{F}(\alpha + \Delta\alpha) = 0$, where $\tilde{F}$ is a first order approximation of F at α. Denoting by $\mathcal{J}(\alpha)$ the matrix $N \times m$ constituted by total gradients of φ_i, $i \in \mathcal{I}$, $m = \mathrm{card}(\mathcal{I})$, w.r.t. α, then we have

$$\Delta\alpha = \left[\mathcal{J}(\alpha) \, \mathcal{J}^T(\alpha) + \lambda I \right]^{-1} \mathcal{J}(\alpha) \left[\bar{\varphi} - \varphi(\alpha) \right] ,$$

where λ is the step length reduction, I is the identity and φ is column of φ_i. Therefore, in order to compute a descend step $\Delta\alpha$, one needs to compute the total (sub)gradients of each $\varphi_i \left(\alpha, y^{(i)}(\alpha) \right)$, $i \in \mathcal{I}$, i.e. to perform a *sensitivity analysis*. The parameter λ is being modified during the minimization process to achieve the convergence. We employed the LEASTSQ subroutine of the MATLAB optimization toolbox, which seems to be a satisfactory implementation of the method, cf. [12].

It has been already mentioned that, because of the projection employed in the definitions of tensions for both types of fibres, the response $\mathbf{y}$ is not differentiable in the classical sense. This becomes actual whenever an active fibre contracts with exactly zero deformation rate, see Fig. 1, or none of the inequalities in Eq. (10) is strict. In such a case, the algorithm of sensitivity analysis given below may fail to provide a correct subgradient, so that a wrong "descent" direction is obtained. According to our experience, however, such situations have been rarely observed. An analogous case has been discussed e.g. in [19] for elastoplasticity. In this section we mention an application of two sensitivity analysis methods: the direct differentiation method (DDM) and the adjoint system method (ASM), see e.g. [10].

6.1. Direct Differentiation Method (DDM)

This method is based on direct computation of the state variable sensitivities $\nabla y^{(t)}$. We consider the extended state problem (32) and define the partial gradients (matrices) of the *state function* $\Phi^{(t)}$,

$$A^{(t)} = \left\{ \frac{\partial \Phi^{(t)}}{\partial y^{(t)}} \right\}_{M \times M} , \qquad W^{(t)} = \left\{ \frac{\partial \Phi^{(t)}}{\partial y^{(t-1)}} \right\}_{M \times M} , \qquad V^{(t)} = \left\{ \frac{\partial \Phi^{(t)}}{\partial \alpha} \right\}_{M \times N} .$$

Differentiating the state equation $\Phi^{(t)}\left(\alpha, y^{(t-1)}, y^{(t)}\right) = 0$, with respect to $\alpha \in \mathbb{R}^N$, we obtain the sensitivity equation with N right hand sides

$$A^{(t)} \nabla y^{(t)} = -\left[V^{(t)} + W^{(t)} \nabla y^{(t-1)}\right], \qquad \text{where} \quad \nabla y^{(0)} = 0, \tag{43}$$

so that the gradient $\nabla y^{(t)}$ of $y^{(t)}$ w.r.t. α (the matrix $M \times N$) can be computed recurrently for $t = 1, 2, \ldots$. The total (sub)gradient of function φ_i employed in Eq. (39) is given by

$$\nabla \varphi_i = \frac{\partial \varphi_i}{\partial \alpha} + \sum_{t=1}^{i} \left(\nabla y^{(t)}\right)^T \frac{\partial \varphi_i}{\partial y^{(t)}}, \tag{44}$$

so that we have

$$\nabla F = \sum_{i \in I} (\varphi_i - \bar{\varphi}_i) \nabla \varphi_i . \tag{45}$$

As will be shown, to solve Eq. (43), the same solver as that for the linear subproblems (38) of the Newton's iterations of the state problem can be used. The matrix $A^{(t)}$ is regular. Its block structure corresponds to that one in Eq. (33).

Remark 5. If the interaction problem described in Section 5 is considered, we introduce the *extended pressure vector* by $\tilde{p} := [p^T, \pi]^T$ and the *extended pressure matrix*, see Eq. (38), by $\tilde{P}^T := [P^T, \hbar]$.

The block structure of columns in matrix $A^{(t)}$ corresponds to the blocks in $\nabla y^{(t)}$,

$$\nabla y^{(t)} = \begin{pmatrix} \nabla u \\ \nabla \tilde{p} \\ \nabla \tau \\ \nabla h \end{pmatrix}^{(t)}, \qquad A^{(t)} = \begin{bmatrix} K^* & \tilde{P}^T & Z & 0 \\ \tilde{P} & 0 & 0 & 0 \\ G & 0 & I & 0 \\ 0 & 0 & -bI & I \end{bmatrix}, \tag{46}$$

where K^* is the stiffness matrix derived from K in Eq. (38); in contrast to K, matrix K^* does not comprise contributions from the tensions in the passive fibres, as these are treated separately in the extended state problem, see Eq. (32). It holds that

$$K = K^* - ZG .$$

For illustration we show the restrictions of matrices G and Z to a finite element e (for brevity the superscript $^{(t)}$ is omitted)

$$[G_e]_{i_{(k,q)}\, j} = \begin{cases} 0 & \text{unloaded,} \\ -(\gamma_\infty \alpha / c)\, \exp\{\kappa \epsilon(\underline{u}) - \epsilon_0^k\}\, [\nu^k \nu^k]|_q : \left[B(\underline{\xi}^q, u)\right]_j^T & \text{loaded,} \end{cases}$$

$$[Z_e]_{j i_{(k,q)}} = \phi^f \phi_f^k \left[B^T(\underline{\xi}^q, u)\right]_j : [\nu^k \nu^k]|_q .$$

Above the index $i_{(k,q)}$ is assigned to the preferential direction of a passive fibre, k, and to the quadrature point $\underline{\xi}^q$.

The system of linear equations (43) can be reduced. For a fixed time level $^{(t)}$ let us denote by r one of the vectors occurring at the right hand side and by ∂y the corresponding sensitivity vector (i.e. the derivative of y w.r.t. one of the identification parameters)

$$r = \begin{pmatrix} r_u \\ \tilde{r}_p \\ r_\tau \\ r_h \end{pmatrix}^{(t)}, \qquad \partial y = \begin{pmatrix} \partial u \\ \partial \tilde{p} \\ \partial \tau \\ \partial h \end{pmatrix}^{(t)}, \tag{47}$$

where by $\tilde{}$ we mean the extension for the interaction problem, as discussed above. Using identity $K = K^* - ZG$, Eq. (43) reduces to

$$\begin{bmatrix} K & \tilde{P}^T \\ \tilde{P} & 0 \end{bmatrix} \begin{pmatrix} \partial u \\ \partial \tilde{p} \end{pmatrix} = \begin{pmatrix} r_u - Z r_\tau \\ \tilde{r}_p \end{pmatrix} . \tag{48}$$

Comparing Eq. (48) with Eq. (38) and taking into account Remark 5, we see, that in both the cases the matrices are identical, so that the same solution procedure can be applied. Having computed ∂u and $\partial \tilde{p}$ the remaining blocks of the sensitivity vector can be obtained using

$$\begin{aligned} \partial \tau &= r_\tau - G\,\partial u\,, \\ \partial h &= r_h + b\,\partial \tau\,. \end{aligned} \tag{49}$$

6.2. Adjoint System Method (ASM)

For derivation and some theory concerning this method we refer the reader to e.g. [19] and to the literature cited therein, or to [10]. We define the *adjoint variables* (vectors) $\omega_{[i]}^{(t)}$ for $i \geq t$, $t \in \{1, \ldots, n\}$, which at the time level (t) are assigned to the function $\varphi_i \left(\alpha, y^{(i)}\right)$, $i \in \mathcal{I}$. The block structure of $\omega_{[i]}^{(t)}$ is as follows (compare with Eq. (47)),

$$\left(\omega_{[i]}^{(t)}\right)^T = \left(\omega_u^T\,,\, \tilde{\omega}_p^T\,,\, \omega_\tau^T\,,\, \omega_h^T\right)_{[i]}^{(t)} .$$

The adjoint variables are computed in backward order for $t = n, n-1, \ldots$ by solving the linear system

$$\left[A^{(t)}\right]^T \cdot \left\{\omega_{[i]}^{(t)}\right\} = \left\{r_{[i]}^{(t)}\right\} \tag{50}$$

with multiple right-hand sides, i.e. $\forall i \in \mathcal{I} \cap \{t, \ldots, n\}$. Each right-hand side vector (r.h.s.) is given by

$$r_{[i]}^{(t)} = \begin{cases} -\dfrac{\partial \varphi_i}{\partial y^{(t)}} & \text{for } i = t\,, \\ -[W^{(t+1)}]^T \omega_{[i]}^{(t+1)} & \text{for } i > t\,. \end{cases} \tag{51}$$

The (sub)gradient of φ_i is computed using the adjoint variables, as follows

$$\nabla \varphi_i = \frac{\partial \varphi_i}{\partial \alpha} + \sum_{t=1}^{i} \left[V^{(t)}\right]^T \omega_{[i]}^{(t)}\,, \tag{52}$$

and ∇F is then obtained by Eq. (45).

The *adjoint equations* are similar in structure to (48) and have the following reduced form,

$$\begin{bmatrix} K & \tilde{P}^T \\ \tilde{P} & 0 \end{bmatrix} \begin{pmatrix} \omega_u \\ \tilde{\omega}_p \end{pmatrix}_{[i]}^{(t)} = \begin{pmatrix} r_u - G^T(b\,r_h + r_t) \\ \tilde{r}_p \end{pmatrix}_{[i]}^{(t)} , \tag{53}$$

where the block structure of vector r corresponds to that of r in Eq. (47). We recall that Eq. (53) has a number of r.h.s. (signed by $[i]$) equal to $\mathrm{card}\{i \in \mathcal{I} \mid i \geq t\}$. The number depends on the time level (t) and on the specific index set $\mathcal{I}$ introduced above, see Eq. (39) and Fig. 5. In analogy with the DDM method, the remaining blocks of ω are computed by

$$\begin{aligned} \omega_\tau &= b\,r_h - Z^T \omega_u + r_t\,, \\ \omega_h &= r_h\,. \end{aligned} \tag{54}$$

It is worth noting that in ASM method the number of r.h.s. in Eq. (53) is independent of the number of identification parameters used, in contrast to DDM method. Therefore, it can be more effective (in comparison with DDM) in such situations when "only few" measurements are made, i.e. when the number $m = \mathrm{card}(\mathcal{I})$ is small. Usually m is large and, thus, DDM is preferred. The comparison of efficiency of ASM and DDM is illustrated in Fig. 6. We remark that if only ∇F was required and not $\nabla \varphi_i$ for each $i \in \mathcal{I}$ then only one adjoint vector would have to be computed at each time level and, thereby, making the ASM approach quite effective.

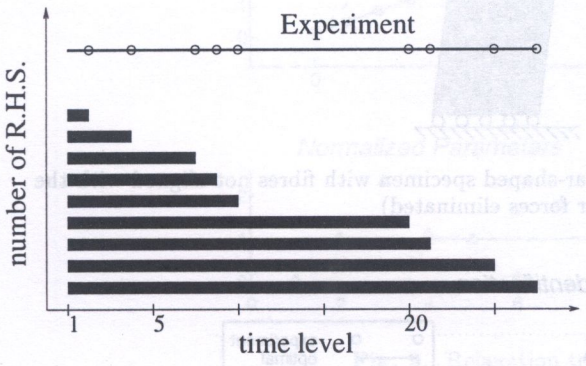

Fig. 5. The number of the r.h.s. vectors (1 to 9) vs. time level in the ASM algorithm for the particular time record of experimental data (the 9 time levels of evaluation indicated by circles)

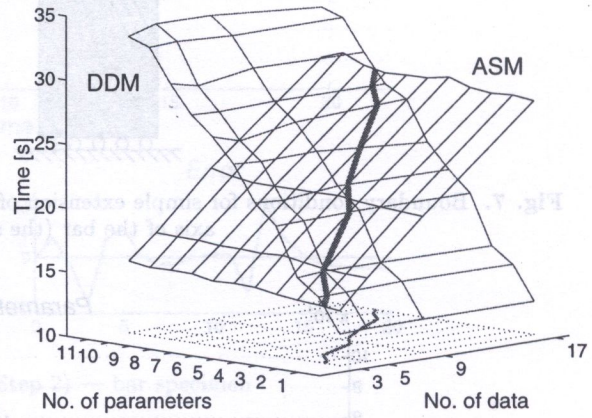

Fig. 6. Efficiency (in CPU time) of sensitivity methods depending on card $\mathcal{I} = 3, 5, 9, 17$; 17 time levels for the state problem

7. Numerical tests

In this section we demonstrate viability of the approach proposed in this paper. So far we have not access to any experimental data describing a particular test which would be accompanied with a relevant information about the microstructure of the specimen. Therefore, by the *"experimental data"* we understand a data defined at discrete time levels which are chosen, as to our knowledge, in accordance with the information provided in literature, cf. [1, 5, 7, 16]. These data are to *be fitted* with a "curve" which is computed by the numerical simulation. Such a curve is being shaped by varying the material parameters during the optimization process.

All numerical computations, including sensitivity analysis, were performed using our special code developed for this purpose. For minimization of the objective functions we applied the standard LEASTSQ subroutine of MATLAB, cf. [12], and adapted it for treating natural box constraints (non-negative stiffness etc.)

7.1. Consistency between hysteresis and relaxation tests

We consider a bar-shaped specimen (in 3D) subjected to stretch program according to Section 6. The Dirichlet boundary conditions prescribed at both the ends of the specimen are illustrated in Fig. 7. The objective function is defined in (41). In the specimen 4 non-parallel systems of passive fibres were considered, two with the "exponential" elastic response (9) and two with the "linear" one, see [17], no activation of muscle considered.

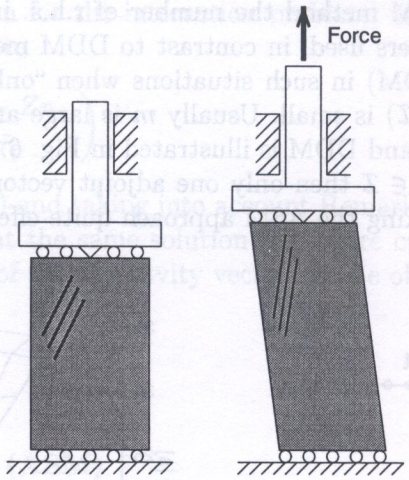

Fig. 7. Boundary conditions for simple extension of a bar-shaped specimen with fibres not aligned with the axis of the bar (the shear forces eliminated)

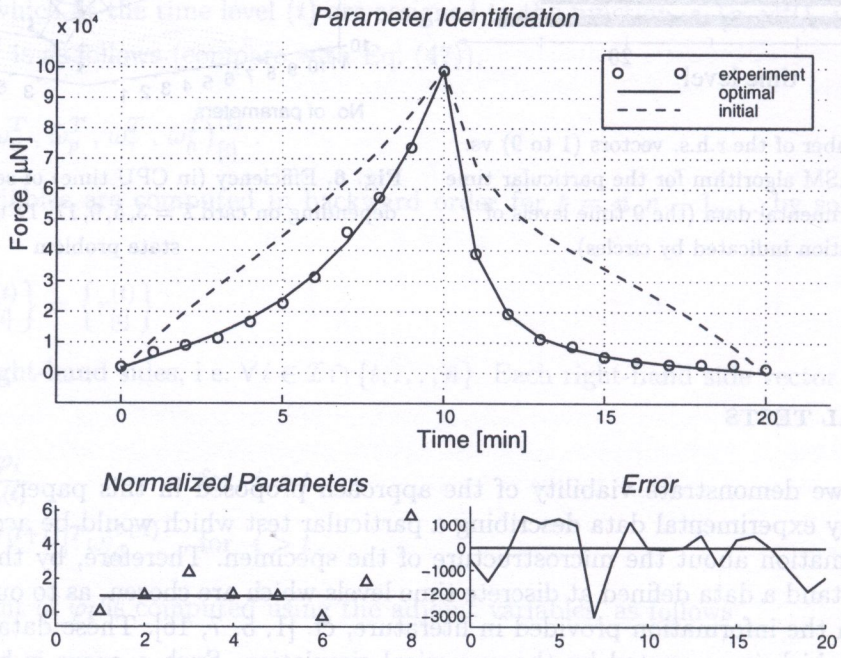

Fig. 8. Hysteresis test (Step 1) — bar specimen

Step 1: First we performed the hysteresis test to get some *optimal* setting of 8 parameters displayed in Fig. 8 in the following order: μ, for matrix, κ, γ_∞, β, γ, $\bar{\epsilon}_0^1$, $\bar{\epsilon}_0^2$ for the "exponential" fibres and γ_∞ for the "linear" ones. In Fig. 8 and in all subsequent, the initial setting is depicted in "Normalized Parameters" box by the solid line, the optimal setting indicated by triangles. The "Error" box shows the discrepancies $\varphi_i\left(\alpha, y^{(i)}\right) - \bar{\varphi}_i$ (see Eq. (39)). The "experiment" data were chosen according to literature, cf. [1, 5, 16], — they were **not precomputed** by our software. Consequently, a relatively significant error in fitting exists. Let us denote this case by "NPData" (as Not Precomputed Data).

Step 2: The *optimal* setting of Step 1 had been used to calculate the relaxation response, which became the *experimental data*. Then identification was tried out, starting from the same initial setting, as in Step 1. As can be observed comparing the normalized parameters displayed in

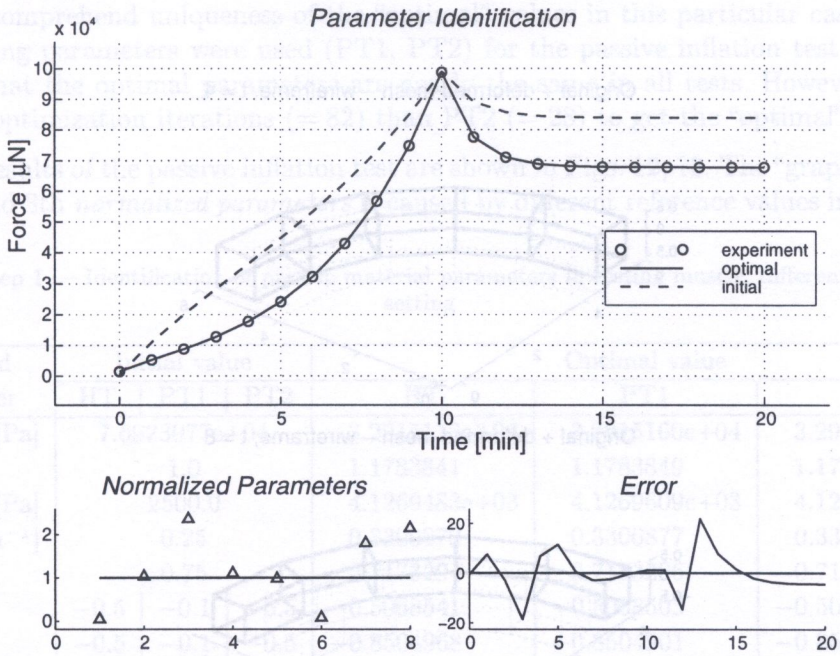

Fig. 9. Relaxation test (Step 2) — bar specimen

Figs. 8 and 9, almost the same optimal setting of the identification parameters was found in both the steps. The only remarkable difference is that in the parameter 8, i.e. γ_∞ of the "linear" fibres. In this case the fitting error was negligible, since the "experiment" data were obtained by our model. Let us denote this case by "PData" (as Precomputed Data).

In this way we verified, that both tests lead to the (almost) same parameters.

7.2. Identification with inflation test

A circular macroscopically homogeneous specimen was being inflated in time increments, as discussed in Section 5. Due to symmetry of the geometry only one quarter was considered for the computation (see Fig. 10). The specimen was reinforced by three systems of fibres — circular muscle fibres (active) (AF), circular (EPF1) and longitudinal (EPF2) passive fibres (exponential model) with volume fractions 0.26, 0.24 and 0.25, respectively. The *fluid pressure* was used to evaluate the objective function (41). The test consisted of two parts:

1. Identification of passive properties (matrix and viscoelastic fibres) with zero AF activation.

2. Identification of muscle fibre properties under full activation while passive properties corresponded to the fixed optimal parameters obtained in Step 1.

Step 1: To have a reasonable objective function values, an auxiliary hysteresis test (HT) with a force objective function chosen according to literature was run on a bar specimen ($\rightarrow$ NPData). Fibre directions were as follows AF: $[-1, 2, 1]^T$, EPF1: $[1, -1, 1]^T$, EPF2: $[0, 0, 1]^T$); the loading force was acting in the direction of the third coordinate axis. Values of the starting parameters are in Table 2. Then the identified parameters (see Fig. 11, Table 2) were used to compute values of the "experimental" fluid pressure time record ($\rightarrow$ PData) for the circular specimen. Hence, in analogy with the example of Section 7.1, one expects the optimal parameters obtained by the inflation test to be almost those of HT.

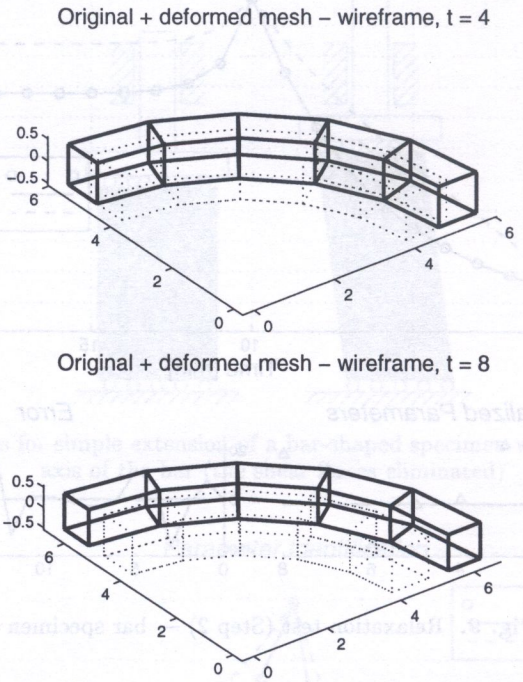

Fig. 10. Inflation test — deformed tube in half (above) and full (bottom) inflated state

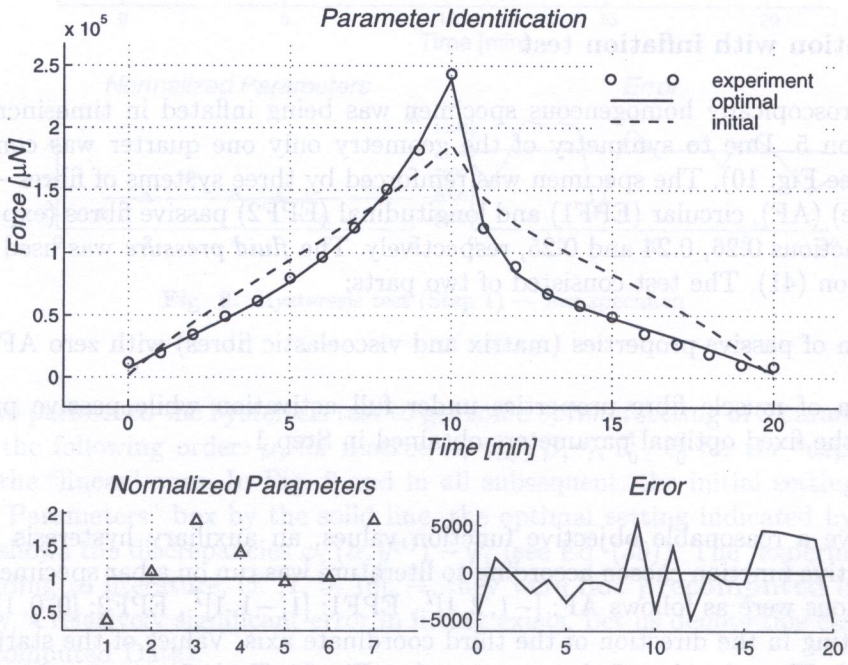

Fig. 11. Auxiliary hysteresis test HT

In order to comprehend uniqueness of the "optimal" values in this particular case, two different sets of starting parameters were used (PT1, PT2) for the passive inflation test. It can be seen in Table 2 that the optimal parameters are nearly the same in all tests. However, PT1 needed much more optimization iterations (= 82) than PT2 (= 28) to get the "optimal" values.

The actual results of the passive inflation test are shown in Figs. 12, 13. The "graphical" difference in the 6th and 8th *normalized parameters* is caused by different reference values in PT1 and PT2.

Table 2. Step 1 — Identification of passive material parameters in resting muscle; different $\bar{\epsilon}_0^k$ at initial setting

Identified parameter		Initial value			Optimal value		
		HT	PT1	PT2	HT	PT1	PT2
1	μ [Pa]	7.6923077e+04			3.2915113e+04	3.2915160e+04	3.2915122e+04
2	κ	1.0			1.1783841	1.1783849	1.1783842
3	γ_∞ [Pa]	2500.0			4.1269483e+03	4.1269609e+03	4.1269517e+03
4	β [min^{-1}]	0.25			0.3300879	0.3300877	0.3300879
5	γ	0.75			0.7173294	0.7173296	0.7173294
6	$\bar{\epsilon}_0^1$	−0.5	−0.1	−0.5	−0.5068541	−0.5068503	−0.5068533
7	$\bar{\epsilon}_0^2$	−0.5	−0.1	−0.5	−0.8504968	−0.8504901	−0.8504955

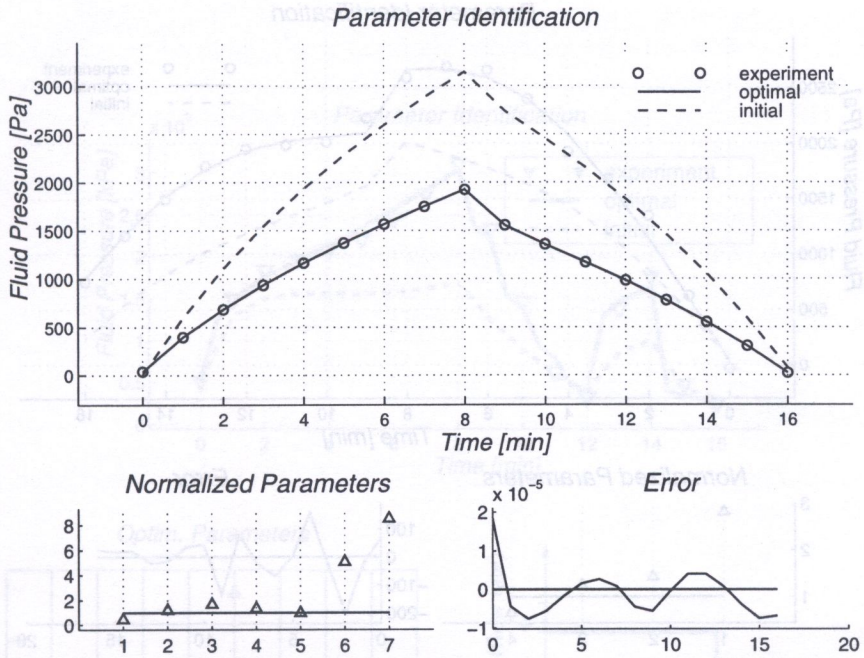

Fig. 12. Inflation test PT1

Step 2: With the passive properties identified, we proceeded to active inflation test (AT). The initial parameters were chosen according to literature. The objective function values (related to the fluid pressure) were obtained by a random perturbation and shift of initial setting (→ NPData). See Table 3 and Fig. 14 for the results. The history of objective function values during the minimization by the LEASTSQ subroutine is depicted in Fig. 15 for the cases with and without the natural box constraint, respectively.

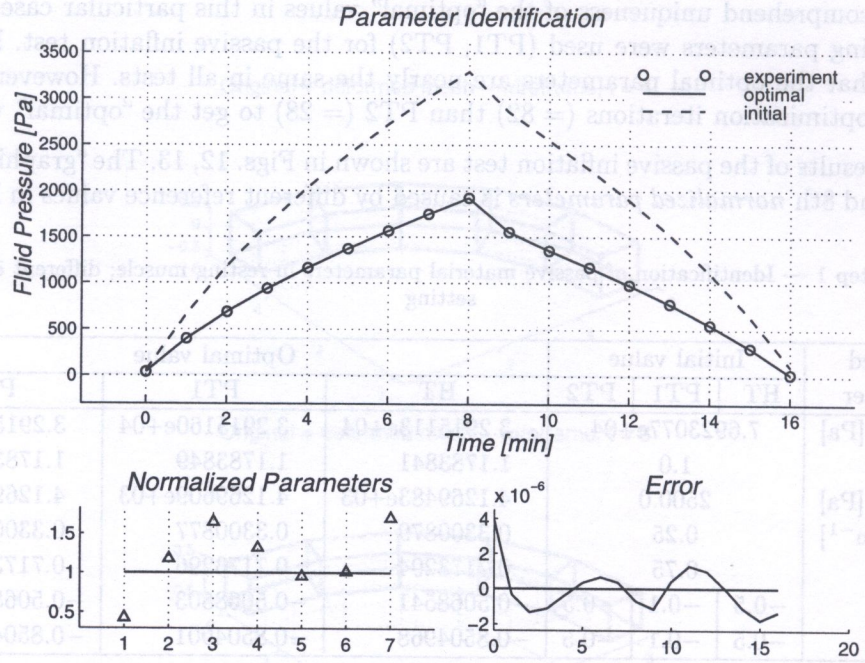

Fig. 13. Inflation test PT2

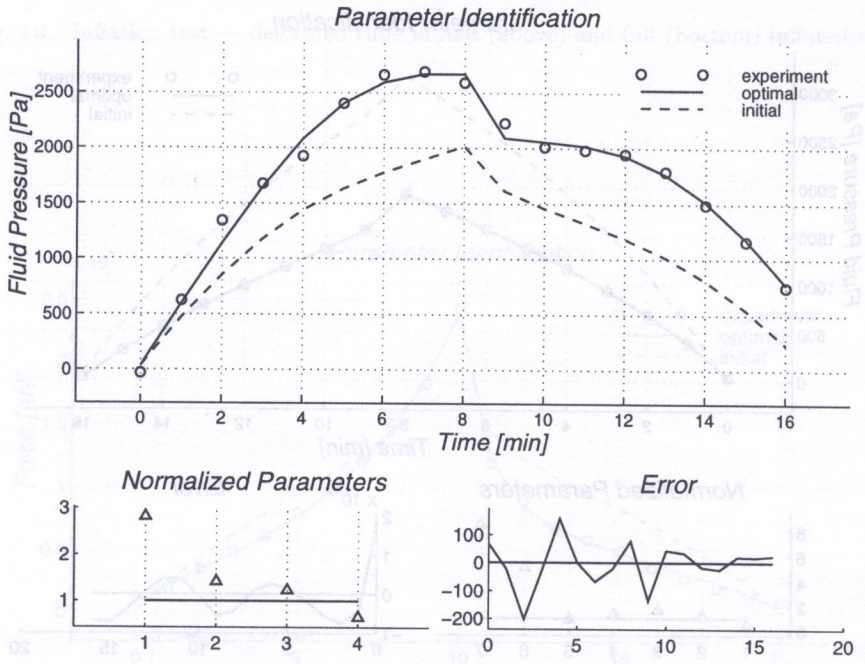

Fig. 14. Inflation test AT — full activated muscle fibres

Table 3. Step 2 — active material parameters

Identified parameter	Initial value	Optimal value
f_{max} [Pa]	1.0e+04	2.8143484e+04
ϵ_{opt}	0.1	0.1418453
s	0.2	0.2472468
ϑ	2.0e+01	1.3048942e+01

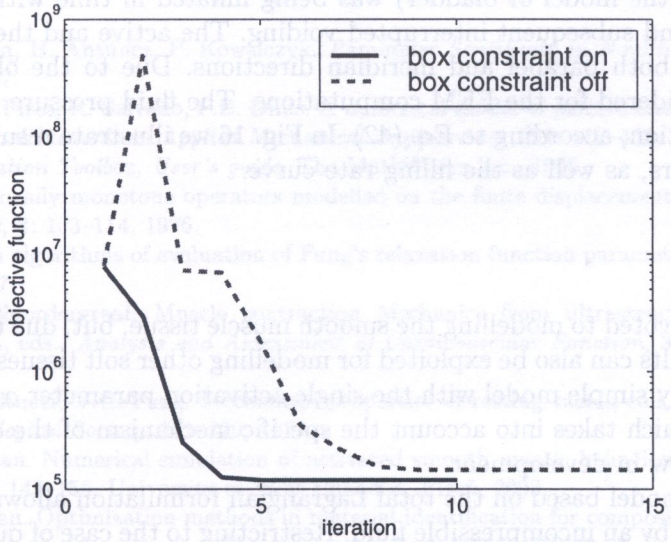

Fig. 15. History of the objective function for the test AT

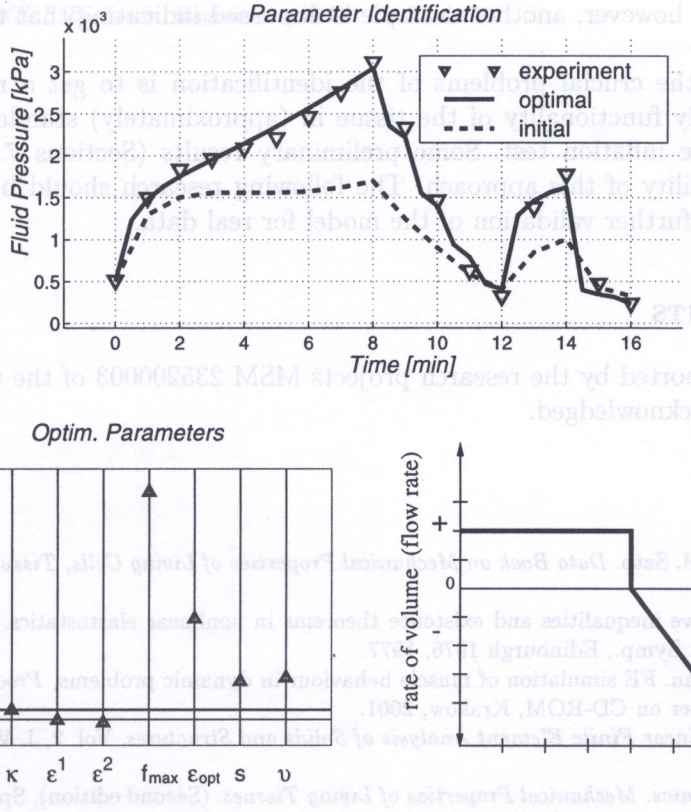

Fig. 16. Identification test based on fluid pressure fitting

7.3. Bladder filling test

A spherical specimen (the model of bladder) was being inflated in time with a given volume rate, simulating the filling and subsequent interrupted voiding. The active and the "exponential" passive fibres were aligned in both parallel and meridian directions. Due to the obvious symmetry only a hemisphere was considered for the FEM computations. The fluid pressure (NPData) was the objective of the identification, according to Eq. (42). In Fig. 16 we illustrate results of the identification of 8 material parameters, as well as the filling rate curve.

8. Conclusions

The present study is devoted to modelling the smooth muscle tissue, but, due to the large complexity of the model, some results can also be exploited for modelling other soft tissues. The muscle fibres are described by a relatively simple model with the single activation parameter α. A more sophisticated model of activation, which takes into account the specific mechanism of the cross-bridge activation in smooth muscle is now in development.

The finite element model based on the total Lagrangian formulation allows alternatively to treat the inflation of a vessel by an incompressible fluid. Restricting to the case of quasi-static deformation (i.e. no inertia forces considered) and due to the appropriate linearization employed, the extended stiffness matrix in Eq. (38) remains symmetric.

The main focus of the paper lies in the material identification and in the related topics of the sensitivity analysis. In the numerical test described in Section 7.2 we considered identification of the passive parameters separately from identification of the active ones, however, we were successful also in cases when all parameters were identified simultaneously, as in Section 7.3. For the particular example of hysteresis and relaxation tests, see Section 7.1, we found consistency in optimal setting of both the tests. In [18], however, another example is discussed indicating that the "optimal" solution may not be unique.

Obviously, one of the crucial problems of the identification is to get a relevant experimental data. In order to study functionality of the tissue in (approximately) standard *in situ* conditions we propose to use the inflation test. Some preliminary results (Sections 7.2 and 7.3) has been obtained proving viability of this approach. The following research should be focussed on testing the identification and further validation of the model for real data.

Acknowledgments

The research was supported by the research projects MSM 235200003 of the Czech Republic. This support is gratefully acknowledged.

References

[1] H. Abé, K. Hayashi, M. Sato. *Data Book on Mechanical Properties of Living Cells, Tissues, and Organs.* Springer-Verlag, Tokyo, 1996.

[2] J.M. Ball. Constitutive inequalities and existence theorems in nonlinear elastostatics. *Nonlin. Anal. Mech.*, **1**: 187–241. Heriot-Watt Symp., Edinburgh 1976, 1977.

[3] R. Cimrman, E. Rohan. FE simulation of muscle behaviour in dynamic problems, *Proceedings of the conference ECCM 2001*, full paper on CD-ROM, Kraków, 2001.

[4] M.A. Crisfield. *Non-linear Finite Element Analysis of Solids and Structures*, Vol. 2, J. Wiley & Sons, Chichester, 1997.

[5] Y.C. Fung. *Biomechanics. Mechanical Properties of Living Tissues.* (Second edition), Springer-Verlag, New York, 1993.

[6] A.C. Guyton, J.E. Hall. *Textbook of Medical Physiology.* W.B. Saunders Company, Philadelphia, 1995.

[7] D.S. Hickey, J.I. Phillips, D.W.L. Hukins. Arrangement of collagen fibrils and muscle fibres in the female urethra and their implications for the control of micturition. *British Journal of Urology*, **54**: 556–561, 1982.

[8] J.D. Humprey, R.K. Stumpf, F.C.P. Yin. Determination of a constitutive relation for passive myocardium. *ASME, J. Biomechanical Eng.*, **112**: 333–346, 1990.

[9] Keener, J. & Sneyd, J.: *Mathematical Physiology. Interdisciplinary Applied Mathematics*, Vol. 8. Springer, New York, 1998.

[10] M. Kleiber, T.D. Hien, H. Antúnez, P. Kowalczyk. *Parameter Sensitivity in Nonlinear Mechanics.* J. Wiley & Sons, Chichester, 1997.

[11] J.A.C. Martins, E.B. Pires, R. Salvado, P.B. Dinis. A numerical model of passive and active behavior of skeletal muscles. *Computational Methods in Applied Mechanical Engineering*, **151**: 419–433, 1998.

[12] *MATLAB - Optimization Toolbox, User's guide.* The MathWorks Inc., 1996.

[13] J. Nečas. Theory of locally monotone operators modelled on the finite displacement theory for hyperelasticity. *Beiträge zur Analysis*, **8**: 103–114, 1976.

[14] I. Nigul, U. Nigul. On algorithms of evaluation of Fung's relaxation function parameters. *Journal of Biomechanics*, **20**: 334–352, 1987.

[15] J.L. Palladino, A. Noordergraaf, Muscle contraction Mechanics from ultrastructural dynamics. In: G.M. Drzewiecki, J.K-J. Li, eds., *Analysis and Assessment of Cardiovascular Function*, 33–57. Springer, New York, 1998.

[16] J.M. Price, P.J. Pattitucci, Y.C. Fung. Mechanical properties of resting taenia coli smooth muscle. *Journal of the American Physiological Society*, 211–220, 1979.

[17] E. Rohan, R. Cimrman. Numerical simulation of activated smooth muscle behaviour using finite elements, In: *Proceedings of UWB*, 143–155. University of West Bohemia, Plzeň, 2000.

[18] E. Rohan, R. Cimrman. Optimization methods in material identification for composite model of resting smooth muscle. In: *Proceedings of the conference Engineering Mechanics 2000*, III/59-64, Svratka 2000.

[19] E. Rohan, J.R. Whiteman. Shape optimization of elasto-plastic structures and continua, *Comp. Meth. Appl. Mech. Eng*, **187**: 261–288, Elsevier, 2000.

[20] J.C. Simo, T.J.R. Hughes. *Computational Inelasticity.* Springer-Verlag, Berlin, 1998.

[21] D.H. Van Campen, J.M. Huyghe, P.H.M. Bovendeerd, T. Arts. Biomechanics of the heart muscle. *Eur. J. Mechanics, A/Solids*, **13**: 19–41, 1994.

[22] P. Vena, R. Contro. A viscoelastic model for anisotropic biological tissues in finite strains. In: *Proceedings of the ECCM '99 Conference*, (on CD-ROM) München, 1999.

[23] G.I. Zahalak, S.P. Ma. Muscle activation and contraction: Constitutive relations based directly on cross-bridge kinetics. *Trans. ASME,J. Biomech. Engineering*, **112**: 52–62, 1990.